Effects of Cyclic Glycopolymers Molecular Mobility on their Interactions with Lectins

Jin, Wenkang
Chemical Engineering, Kyushu University

Nagao, Masanori
Faculty of Engineering, Kyushu University

Kumon, Yusuke
Chemical Engineering, Kyushu University

Matsumoto, Hikaru
Chemical Engineering, Kyushu University

他

出版情報：ChemPlusChem, pp.e202400136-, 2024-03-27. Wiley
バージョン：
権利関係：

RESEARCH ARTICLE

Effects of Cyclic Glycopolymers Molecular Mobility on their Interactions with Lectins

Wenkang Jin,[a] Masanori Nagao,*[a] Yusuke Kumon,[a] Hikaru Matsumoto,[a] Yu Hoshino,[b] and Yoshiko Miura*[a]

[a] Dr. Masanori Nagao, Prof. Yoshiko Miura
Department of Chemical Engineering
Kyushu University
744 Motooka, Nishi-ku, Fukuoka, Japan
E-mail: nagaom@chem-eng.kyushu-u.ac.jp ; miuray@chem-eng.kyushu-u.ac.jp

[b] Prof. Yu Hoshino
Department of Applied Chemistry
Kyushu University
744 Motooka, Nishi-ku, Fukuoka, Japan

Supporting information for this article is given via a link at the end of the document.

Abstract: Cyclic polymers, which are found in the field of biopolymers, exhibit unique physical properties such as suppressed molecular mobility. Considering thermodynamics, the suppressed molecular mobility of cyclic polymers is expected to prevent unfavorable entropy loss in molecular interactions. In this study, we synthesized cyclic glycopolymers carrying galactose units and investigated the effects of their molecular mobility on the interactions with a lectin (peanut agglutinin). The synthesized cyclic glycopolymers exhibited delayed elution time on size exclusion chromatography and a short spin–spin relaxation time, indicating typical characteristics of cyclic polymers, including smaller hydrodynamic size and suppressed molecular mobility. The hemagglutination inhibition assay revealed that the cyclic glycopolymers exhibited weakened interactions with peanut agglutinin compared to the linear counterparts, attributable to the suppressed molecular mobility. Although the results are contrary to our expectations, the impact of polymer topology on molecular recognition remains intriguing, particularly in the context of protein repellent activity in the biomedical field.

Introduction

Biomacromolecules such as DNA and proteins possess well-defined structures and exhibit remarkable functions, including molecular interactions. For example, antibodies and enzymes recognize antigens and substrates, respectively, through precise arrangement of functional groups, rendering them indispensable in our vital activities. Replicating such precise structures and functions of natural biomolecules using synthetic polymers is a significant challenge in polymer science.[1] Synthetic polymers can utilize a broader range of monomers than biomacromolecules, providing opportunities to create novel nanomaterials with properties surpassing those of biomolecules. The development of precision polymerization techniques, such as living polymerization, has enabled the synthesis of polymers with relatively controlled structures, including molecular weight, monomer sequence, and topology.[2] This advancement has sparked research into mimicking the three-dimensional structures and functions of biomacromolecules.[3]

Molecular recognition is a prevalent phenomenon among biomolecules within living organisms. For example, glycoconjugates on the cell surface bind to specific carbohydrate-binding proteins (lectins), playing a crucial role in cell-to-cell communication, cancer metastasis, and the infection of pathogens like viruses and toxins.[4] This form of molecular recognition, termed carbohydrate–protein interactions, holds promise for applications in novel biomaterials.[5] Moreover, many lectins possess multiple binding sites for carbohydrates, allowing for multivalent binding that compensates for the inherent weakness of carbohydrate–protein interactions.[6,7] Glycopolymer is one material capable of exhibiting multivalent interactions with lectins. Beyond the multivalency of carbohydrate units in the side chains, the design of polymer structures can further enhance interactions with target lectins, paving the way for the development of biosensors and pathogen inhibitors. [8]

The interactions between biomolecules are commonly interpreted using Gibbs free energy ($\Delta G = \Delta H - T\Delta S$).[9–11] Formation of bonds between the recognition site of proteins and a ligand releases heat, resulting in a gain of enthalpy (ΔH, which is favorable for interactions). However, the mobility of ligand molecules is constrained upon binding to the target, causing entropy loss (ΔS, which is unfavorable for interactions).[12–15] Therefore, when designing the structure of a multivalent ligand, it is crucial not only to display the multiple functional groups to increase enthalpy but also to control the overall mobility (flexibility) of the ligand molecules.[16] Several studies have addressed the design of synthetic polymer ligands considering their molecular mobility.[17,18] Our group has also reported that the interactions of glycopolymers with concanavalin A depended on the mobility of the carbohydrate units in the side chains.[19] However, methods to control the mobility of synthetic polymers are further required

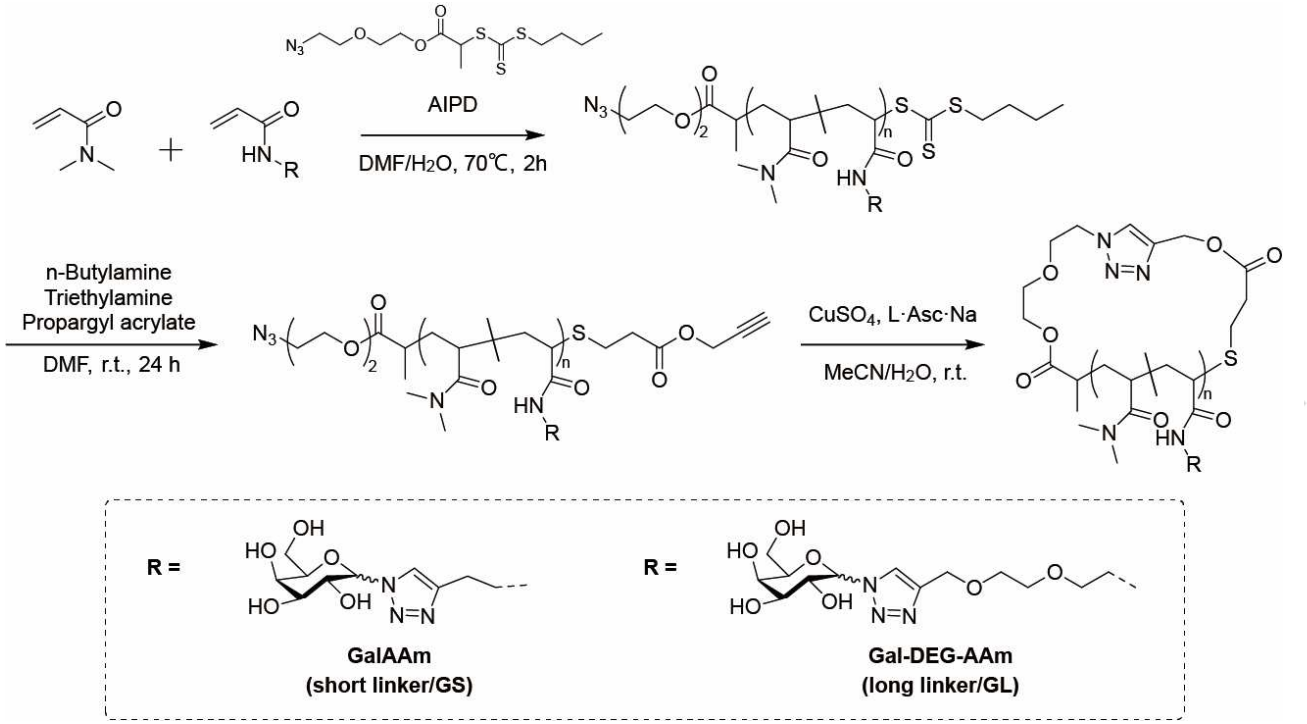

Figure 1. Synthetic scheme for the cyclic glycopolymers by a combination of RAFT polymerization and copper-catalysed azide-alkyne cycloaddition.

because the freedom of the polymer terminals is high in solution, leading to significant entropy loss upon binding.

Cyclic polymers, characterized by the lack of polymer terminals and notable differences in aspects such as structure, mechanics, and thermodynamics compared to linear structures, exhibited suppressed mobility, as indicated in their high glass transition temperature (T_g).[40–42] The advantages stemming from the geometry of ring-shaped structures have been extensively reported in natural cyclic peptides, showcasing benefits ranging from stability to various functionalities.[43] For instance, Grossmann and co-workers stabilized the physiological activity conformation in protein-protein interactions by circulating peptides, thereby enhancing affinity and activity with the target.[44,45] However, studies on the correlation between the physical properties and the interactions of cyclic glycopolymers with target lectins remain limited.[46–48]

Herein, we investigated the effects of the molecular mobility of cyclic glycopolymers on the interactions with a target protein. Our hypothesis was that the suppressed mobility of cyclic glycopolymers would mitigate the entropy loss associated with binding to the target protein, leading to thermodynamic advantages. Furthermore, we explored the impact of flexibility in the side chains displaying carbohydrates. The synthesis of cyclic glycopolymers was achieved through a combination of living radical polymerization and copper-catalyzed azide-alkyne cycloaddition (CuAAC), allowing for precise structural design.[48]

Results and Discussion

Preparation of Linear Precursor of Glycopolymers by RAFT Polymerization

Telechelic glycopolymers with azide and alkyne groups at the polymer terminals were prepared as linear precursors for the cyclic glycopolymers (Figure 1). Glycopolymers carrying galactose units were synthesized by reversible addition–fragmentation chain transfer (RAFT) polymerization with *N,N*-dimethylacrylamide (DMA) and acrylamide derivatives containing galactose units. To assess the effects of carbohydrate mobility in side chains, two types of carbohydrate monomers with different linker structures were prepared. Galactose acrylamide (GalAAm) featured an ethylene unit (shorter linker, abbreviated as **GS**) between the amide and galactose, while galactose-DEG-acrylamide (Gal-DEG-AAm) included two additional EG units (longer linker, abbreviated as **GL**). An azide group was introduced to the "R" group of the RAFT agent (AEBCP) in accordance with previous reports.[26] Various glycopolymers were synthesized with different compositions, such as carbohydrate unit ratio, degree of the polymerization (DP), and monomer structures (Table 1). Detailed conditions are provided in the Supporting Information (Table S1). Monomer conversions exceeded 83% for all polymerization conditions, as determined by ^{1}H NMR (Table 1). The incorporated ratios of galactose units matched the feed ratios. Size exclusion chromatography (SEC) analysis revealed that the relative molecular weights (M_n) of the glycopolymers corresponded to the DP, with dispersity (M_w/M_n) narrower than 1.37 (Table 1 and Figure S1). These results demonstrate the successful synthesis of glycopolymers for the linear precursors through controlled radical polymerization.

Preparation of Telechelic Glycopolymers with Azide and Alkyne by Michael Addition Reaction

To synthesize the telechelic polymer precursors for the cyclization reaction, the trithiocarbonate groups at ω-terminals were converted to alkynyl groups using a one-pot procedure involving aminolysis with *n*-butylamine and a Michael addition reaction to propargyl acrylate (Figure 1). Detailed conditions are provided in the Supporting Information (Table S2). The removal of the trithiocarbonate group was confirmed by UV measurement and ^{1}H NMR analysis. The absorbance peak at 310 nm associated with the trithiocarbonate group, along with the proton peak corresponding to the methyl group of RAFT terminal (-$C_3H_6CH_3$) at 0.9 ppm in D_2O, disappeared (Figure S2). Moreover, the addition of propargyl acrylate to the polymer terminal was confirmed by ^{1}H NMR using DMSO-d_6. The proton peak of the methylene unit adjacent to the alkyne unit appeared at 4.8 ppm in DMSO-d_6 (Figure S16) Although other protons derived from galactose units overlapped, the integration value of protons around 4.8 ppm increased after the Michael addition reaction (Figure S24–29). This result indicated the successful introduction of the alkyne group into the polymer ω-terminals. It is noteworthy that SEC chromatographs did not change after the reaction, indicating the absence of disulfide byproducts during aminolysis (Figure S1). These results demonstrate the successful synthesis of telechelic glycopolymers containing azide and alkyne groups at polymer terminals.

Table 1. Properties of RAFT polymerization for glycopolymers[a].

Polymers[b]	Target DP	Conv. (%)[c]	DP of **D**[c]	DP of **GS** (**GL**)[c]	Carbohydrate ratio [mol%][c]	M_n (g/mol)[d]	M_w/M_n [d]
$D_{45}GS_5$	50	92	45	5	10	4,400	1.14
$D_{35}GS_{15}$	50	88	33	13	28	4,400	1.37
$D_{56}GS_{24}$	80	83	48	19	28	7,700	1.30
$D_{45}GL_5$	50	89	45	4	9	4,400	1.21
$D_{35}GL_{15}$	50	>99	43	19	31	7,800	1.23
$D_{56}GL_{24}$	80	>99	66	29	31	13,100	1.20

[a] Monomer concentration of each polymerization was 2 mol/L. [b] **D**, **GS**, and **GL** abbreviate *N,N*-dimethylacrylamide, galactose acrylamide, and galactose-DEG-acrylamide, respectively. [c] Monomer conversion (Conv.), degree of polymerization (DP), and carbohydrate ratio were determined from ^{1}H NMR. [d] Relative molecular weight (M_n) and dispersity (M_w/M_n) were determined by SEC analysis calibrated with polymethylmethacrylate (PMMA) standards (eluent: 10 mM LiBr in DMF).

Preparation of Cyclic Glycopolymers by Ring-closure Strategy via CuAAC reaction

The ring-closure reaction was accomplished via a CuAAC reaction under highly diluted aqueous conditions to minimize the formation of oligomeric byproducts. This highly dilution was achieved using pseudo high-dilution methods, involving the constant rate addition of the linear precursor to the batch.[27] After the reaction, the products underwent purification via dialysis and filtration to remove the copper catalyst. To assess the progress of the CuAAC reaction, the obtained polymers were analyzed using FT-IR measurements. The peak corresponding to the azide group at 2100 cm^{-1} decreased after the reaction, indicating the progress of the CuAAC reaction (Figure 2a and S3). However, SEC chromatograms of the dialyzed samples displayed bimodal peaks (Figure 2b and S4). The peak with a longer elution time compared to that of the linear precursors signified the production of the desired cyclic polymers, as the smaller hydrodynamic size of cyclic polymers typically results in a delay in elution time. The other peak with a shorter elution time appears to stem from oligomeric byproducts with higher molecular weight, which were formed during the ring-closure reaction even under the highly diluted conditions.

To purify the cyclic polymers, the oligomeric byproducts were removed by cycled SEC separation (the chromatograms are shown in the Supporting Information; Figure S5–S10). The purified cyclic glycopolymers exhibited a unimodal distribution with a delayed elution of peak compared to the precursors, which is a typical characteristic of cyclic polymers[20a] (Figure 2b and S11). These results support the successful separation of the desired cyclic glycopolymers.

The successful CuAAC reaction would form one triazole ring in the polymer main chain per one cyclic polymer. Although the glycopolymers already contained triazole rings in the side chains, the presence of the newly formed triazole ring in the polymer main chain was investigated using ^{1}H NMR. In D_2O, the main peaks of triazole rings of **GS** and **GL** appear at 8.1 and 8.4 ppm, respectively.

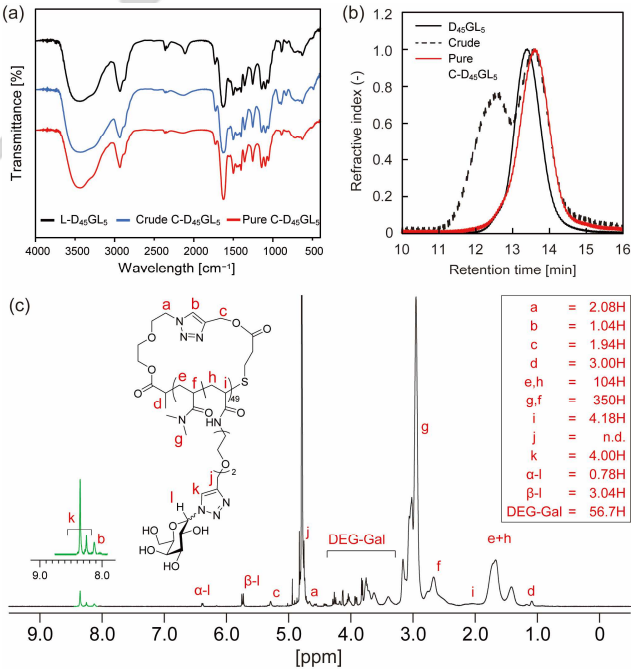

Figure 2. Results of preparation of the cyclic glycopolymer (**C-$D_{45}GL_5$**). (a) FT-IR spectra of linear glycopolymer (black line), crude cyclic glycopolymer (blue line), and purified cyclic glycopolymer (red line), respectively. (b) SEC chromatograms of linear glycopolymer (black line), crude cyclic glycopolymer (dashed line), and purified cyclic glycopolymer (red line), respectively. The eluent was DMF with 10 mM LiBr. The system was calibrated with polymethylmethacrylate standards. (c) ^{1}H NMR spectrum of purified **C-$D_{45}GL_5$** in D_2O.

This difference in chemical shift arises from the adjacent structures of the triazole rings. For the glycopolymers containing **GL**, a small but distinct peak appeared at 8.1 ppm (peak of *b* in Figure 2c for **C-D$_{45}$GL$_5$**, and the other spectra are shown in Figure S33–35). While the peak was not identified for the glycopolymers containing **GS** due to overlap with the triazole rings in the side chains (Figure S30–32), the peak at 8.1 ppm was assigned as a newly formed triazole ring resulting from the cyclization reaction.

Characterization of Linear and Cyclic Glycopolymers

The physical properties of the synthesized linear and cyclic glycopolymers were characterized using differential scanning calorimetry (DSC), spin-spin (T_2) relaxation time by ^{1}H NMR, and dynamic light scattering (DLS). DSC measurements were conducted in the range of 30 to 180°C for two cycles, and the T_g values were determined in the second cycle (Table 2 and Figure S12). Typically, cyclic polymers exhibit higher T_g values than their corresponding linear polymers due to the suppressed mobility of the main chains. The T_g values of the synthesized cyclic glycopolymers were indeed higher than those of the linear precursors, confirming the successful synthesis and purification of cyclic structures.

The glass transition temperature is crucial for evaluating polymer mobility in bulk states. However, for glycopolymers, it is essential to assess their mobility in solution because the interactions with lectins occur in aqueous environments. Therefore, T_2 relaxation times of the glycopolymers were measured at chemical shifts of 1.35 and 5.56 ppm, corresponding to the protons of the main chain and the proton of the anomeric position of galactose in the side chain. Longer T_2 relaxation times indicate higher mobility of the molecules.[3i, 28–30] As anticipated, the extension of the linker structure in the side chains with diethylene glycol units for **D$_{45}$GL$_5$**, **D$_{35}$GL$_{15}$**, and **D$_{56}$GL$_{24}$** resulted in longer T_2 relaxation times at 5.56 ppm (Figure 3d and Table 2), indicating increased mobility of the carbohydrate units in the solution. Additionally, almost all cyclic glycopolymers exhibited shorter T_2 relaxation times than their linear counterparts (Figure 3). In DLS measurements, almost all cyclic glycopolymers demonstrated smaller hydrodynamic diameters (D_h) than the linear precursors except **C-D$_{56}$GS$_{24}$** and **C-D$_{56}$GL$_{24}$** (Table 2, Figure S13 and S14). These results indicate that the molecular mobility of the glycopolymers was suppressed by the cyclization of the main chains.

Table 2. Physical properties of linear and cyclic glycopolymers.

Polymers	T_2 $^{1.35\ ppm}$ [a] [ms]	T_2 $^{5.56\ ppm}$ [a] [s]	T_g [°C]	D_h [b] [nm]
D$_{45}$GS$_5$	45 ± 1.4	0.39 ± 0.03	121.5	3.85 ± 0.19
C-D$_{45}$GS$_5$	38 ± 0.2	0.23 ± 0.01	146.3	3.58 ± 0.21
D$_{35}$GS$_{15}$	37 ± 1.8	0.32 ± 0.02	151.7	4.68 ± 0.37
C-D$_{35}$GS$_{15}$	26 ± 0.7	0.30 ± 0.01	157.2	3.96 ± 0.08
D$_{56}$GS$_{24}$	29 ± 0.9	0.31 ± 0.03	157.2	4.99 ± 0.47
C-D$_{56}$GS$_{24}$	23 ± 0.8	0.29 ± 0.02	163.6	5.38 ± 0.24
D$_{45}$GL$_5$	44 ± 1.0	0.62 ± 0.04	104.3	4.50 ± 0.07
C-D$_{45}$GL$_5$	42 ± 1.7	0.68 ± 0.01	116.3	3.65 ± 0.14
D$_{35}$GL$_{15}$	30 ± 0.4	0.54 ± 0.2	110.1	4.94 ± 0.22
C-D$_{35}$GL$_{15}$	28 ± 0.7	0.48 ± 0.03	112.9	4.90 ± 0.22
D$_{56}$GL$_{24}$	26 ± 0.3	0.52 ± 0.01	116.1	5.80 ± 0.13
C-D$_{56}$GL$_{24}$	29 ± 1.3	0.46 ± 0.01	120.5	6.67 ± 0.27

[a] T_2 relaxation time of the main chain protons and the sugar anomeric protons in the polymer side chains were acquired at 1.35 and 5.56 ppm in ^{1}H NMR spectra, respectively (D_2O). [b] Hydrodynamic diameter (D_h) was measured by DLS in PBS (-) buffer (1 g/L).

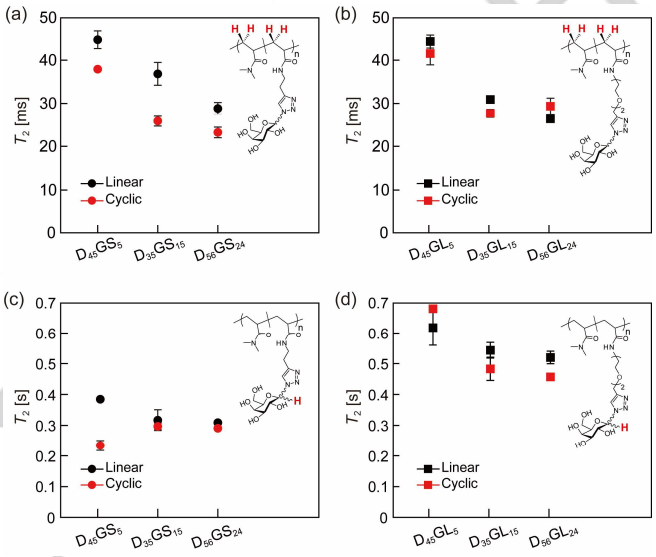

Figure 3. T_2 relaxation times of the glycopolymers containing **GS** (**D$_{45}$GS$_5$**, **D$_{35}$GS$_{15}$**, and **D$_{56}$GS$_{24}$**) at 1.35 ppm (a) and 5.56 ppm (c), respectively. T_2 relaxation time of the glycopolymers containing **GL** (**D$_{45}$GL$_5$**, **D$_{35}$GL$_{15}$**, and **D$_{56}$GL$_{24}$**) at 1.35 ppm (b) and 5.56 ppm (d), respectively.

Interaction of Synthesized Glycopolymers with a Lectin by a hemagglutination inhibition assay

The interactions of the glycopolymers with the target lectin were evaluated through a hemagglutination inhibition (HI) assay. Peanut agglutinin (PNA), a tetrameric lectin with an affinity for galactose units, induces the aggregation of red blood cells (RBCs) by binding to the galactose units on the surface of RBCs. The synthesized glycopolymers carrying galactose units bound to PNA and inhibited the RBC aggregation. The minimum polymer concentration required for HI was defined as K_i, where lower K_i values indicate stronger interactions. To compare interactions of the glycopolymers containing carbohydrate units in the various ratios, the K_i values are presented in terms of galactose unit concentration (Table 3 and Figure 4). For the the glycopolymers containing **GS**, the K_i values were 2.3, 4.8, and 2.5 μM for the linear structures (**D$_{45}$GS$_5$**, **D$_{35}$GS$_{15}$**, and **D$_{56}$GS$_{24}$**, respectively)

and 781, 617, and 105 μM for the cyclic structures (**C-D$_{45}$GS$_5$**, **C-D$_{35}$GS$_{15}$**, and **C-D$_{56}$GS$_{24}$**, respectively). In contrast, the glycopolymers containing **GL** showed the higher K_i values than those containing **GS** (23, 290, 49, and 974 μM for **D$_{45}$GL$_5$**, **D$_{35}$GL$_{15}$**, **D$_{56}$GL$_{24}$**, and **C-D$_{56}$GL$_{24}$** respectively). K_i values for **C-D$_{45}$GL$_5$** and **C-D$_{35}$GL$_{15}$** were higher than the maximum concentration (K_i > 1.5 mM), which is expressed as "n.d." (not determined) in Figure 4.

The effect of the linker structures on the interactions is discussed by comparing the **GS** and **GL** polymer series. The higher K_i values for the glycopolymers with the long linker structure (**GL**) indicated weaker interactions with PNA than the corresponding glycopolymers with the short linker structure (**GS**), regardless of the molecular topology. Considering the lower mobility of the carbohydrate units in **GS** compared to **GL** (Figure 3c, d), the suppressed mobility of carbohydrate units in the side chains of **GS** appeared advantageous for the interaction, possibly avoiding entropy loss caused by the intermolecular binding. Additionally, the effects of the carbohydrate unit ratio varied for each linker structure. Among the glycopolymers containing **GS**, both linear and cyclic glycopolymers with the carbohydrate units at 10 mol% (**D$_{45}$GS$_5$** and **C-D$_{45}$GS$_5$**) exhibited the K_i values close to those of their counterparts with 30 mol% carbohydrate units (**D$_{35}$GS$_{15}$** and **C-D$_{35}$GS$_{15}$**). In contrast, **D$_{45}$GL$_5$** exhibited the K_i value 10 times lower than **D$_{35}$GL$_{15}$**. This discrepancy implies that the galactose units with a long linker structure (**GL**) in the glycopolymers were not fully engaged in the interaction with PNA. These results suggest that the molecular mobility of functional groups in polymer ligands should be suppressed with short linker structures.

Table 3. The K_i values of the glycopolymers against PNA[a].

Polymers	K_i (μM)	
	Linear	Cyclic
D$_{45}$GS$_5$	2.3 ± 0.7	781 ± 368
D$_{35}$GS$_{15}$	4.8 ± 1.5	617 ± 194
D$_{56}$GS$_{24}$	2.5 ± 0.8	105 ± 0
D$_{45}$GL$_5$	23 ± 0	n.d.[b]
D$_{35}$GL$_{15}$	290 ± 91	n.d.[b]
D$_{56}$GL$_{24}$	49 ± 0	974 ± 663

[a] K_i indicates the minimum galactose concentration required for HI activity (μM). [b] N.D. indicates "not determined" (no activity was observed in the concentration range).

The effect of polymer main chain mobility on the interaction was investigated by comparing the linear and cyclic glycopolymers. The K_i values of the cyclic glycopolymers ranged from 105 to 974 μM, higher than those of the linear glycopolymers (2.3–15.2 μM). Despite the expectation that the cyclic polymers, with their suppressed molecular mobility, would exhibit enhanced interactions, they demonstrated higher K_i values than their corresponding linear counterparts across various structural

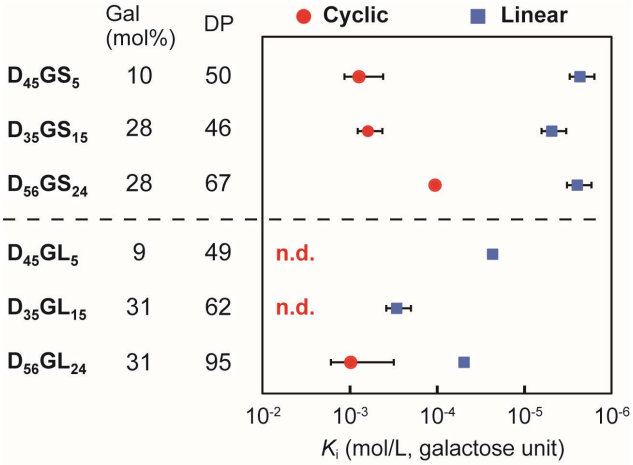

Figure 4. Results of hemagglutination inhibition assay presented in carbohydrate unit concentration. Blue squares and red circles indicate the linear and cyclic glycopolymers. DP indicates the degree of polymerization of each glycopolymer.

parameters such as linker structures, carbohydrate unit ratios, and molecular weights. This indicates weaker interactions of the cyclic glycopolymers with PNA. Considering that PNA has four carbohydrate binding sites and a multivalent binding mode is expected, the larger molecular weight of glycopolymers should facilitate bridging the multiple binding sites on PNA (the distance between two binding sites is ca. 6.8 nm).[31] However, the K_i value of **C-D$_{56}$GS$_{24}$** (974 μM) was higher than that of **D$_{45}$GS$_5$** (2.3 μM), despite **C-D$_{56}$GS$_{24}$** having the larger hydrodynamic diameter than **D$_{45}$GS$_{24}$** (5.38 and 3.85 nm, respectively in Table 2). This result suggests that the negative impact on the interactions stemmed from the suppressed molecular mobility of the cyclic glycopolymers, rather than their hydrodynamic sizes. Given the reports about effective ligand molecules using rigid protein structures,[32,33] a positive impact of the suppressed mobility of the polymer structure on molecular interactions would be observed only when multiple functional groups are arranged precisely for the target molecular structure. Otherwise, a flexible polymer structure capable of achieving an optimal arrangement of functional groups appears advantageous for interactions. While the suppressed mobility of the cyclic glycopolymers proved disadvantageous for the molecular interaction, the effect of the molecular topology on molecular recognition remains interesting. For example, cyclic poly(ethylene glycol) interacting with gold nanoparticles has been reported to enhance blood circulation.[34] The repellent activity of cyclic glycopolymers, designed to bind to lectins in linear structures, could lead to new biological applications.

Conclusions

In summary, we synthesized various glycopolymers carrying galactose and systematically investigated the effects of polymer topology on their biological function. The glycopolymers were varied in terms of carbohydrate unit ratio, molecular weight, and linker structure in the side chains. Cyclic glycopolymers were obtained through a ring-closure reaction of the telechelic

glycopolymers displaying azide and alkyne groups at the polymer terminals. Purification of oligomeric byproducts, arising from intermolecular polymer conjugation, was achieved using a recycle SEC system. The purified cyclic glycopolymers exhibited typical properties of cyclic polymers, such as smaller hydrodynamic size, higher glass transition temperature and suppressed molecular mobility. The T_2 relaxation times of carbohydrate units with a diethylene glycol linker were longer than that with a short linker structure, indicating the molecular mobility of carbohydrate units depends on linker length. In the Hi assay, the cyclic glycopolymers showed weakened interactions with PNA compared to the linear precursors. Interestingly, the weakening of the interactions in the cyclic glycopolymers was attributed to the suppressed molecular mobility of the polymer main chains, while the lower molecular mobility of carbohydrate units with the short linker structure proved advantageous for the interactions with PNA. Consequently, in the synthesis of polymer ligands for strong interaction with target pathogens, it is crucial to design molecular mobility considering which parts should be rigid or flexible. Although the results in this work contradicted our initial expectation, the topological effect of cyclic polymers has gained attention in the biological field. This work would lead to the development of novel biomaterials with high repelling property in physiological conditions.

Experimental Section

Materials and Methods

The following chemical agents were purchased from commercial sources and were used as received except the notion: Ttriethylamine (TEA, 99%), sodium ascorbate (L·Asc·Na, 98%), 2,2'-azobis[2-(2- imidazolin-2-yl)propane] dihydrochloride (AIPD, 98%), tris[(1-benzyl-1H-1,2,3-triazol-4-yl)methyl]amine (TBTA, 97.0 %), hydroquinone (99%), lithium bromide (LiBr, 99%) and *N,N*-dimethylacrylamide (DMA, 99%) were purchased from Tokyo Chemical Industry (Tokyo, Japan). Copper(II) sulfate ($CuSO_4$), *n*-butylamine (98%), and phosphate-buffered saline (PBS) solution were purchased from Wako Pure Chemical Industries (Osaka, Japan). Propargyl acrylate (98%) was purchased from Sigma Aldrich (St. Louis, USA). Peanut agglutinin (PNA) was purchased from Vector laboratories, Inc. Blood cell suspension from a rabbit was purchased from Cosmo Bio Co. (Tokyo, Japan). 2-(2-azidoethoxy)ethyl 2-(((butylthio)carbonothioyl)thio)propanoate (AEBCP)[26], galactose acrylamide (GalAAm)[35], galactose azide[35], and 2-[2-(2-propynyloxy)ethoxy]ethyl acrylamide[8e] were synthesized referring the previous reports. Commercial monomers including the radical inhibitor were purified by passing through an alumina column prior to use.

Proton nuclear resonance (^{1}H NMR) spectra was recorded on a JEOL-ECP400 spectrometer (JEOL, Tokyo, Japan) using DMSO-d_6 or D_2O as a solvent. The sample concentration was 10 g/L for all polymers. The spin–spin (T_2) relaxation times were measured using the Carr-Purcell-Meiboom-Gill (CPMG) pulse sequence. The delay time was 10 s, which is 5 times longer than T_1. Relaxation data were analyzed using the JEOL Delta software package. The measurement was triplicated for one data (three spectra were obtained). When using D_2O as a solvent, the peak of water was removed by a presaturation mode. Size exclusion chromatography (SEC) with organic solvent was performed on a HLC-8320 GPC Eco-SEC equipped with a TSKgel Super AW guard column and TSKgel Super AW (4000 and 2500) columns (TOSOH, Tokyo, Japan). The SEC analyses were performed at a flow rate of 0.5 mL/min by injecting 20 µL of a polymer solution (2 g/L) in DMF with 10 mM LiBr. The SEC system was calibrated with a polymethylmethacrylate standard (Shodex). All the samples for SEC analysis were previously filtered through a 0.45 µm filter. UV-vis spectra were recorded at room temperature using an Agilent 8453 spectrophotometer (Agilent Technologies, Santa Clara, CA, USA). Fourier transform infrared (FT-IR) spectra were recorded on a JASCO FT/IR4700 (JASCO, Japan). Polymer purification was performed using a recycling SEC system (LaboACE LC-7080) equipped with JAIGEL-GS310/-P1. Dynamic light scattering (DLS) measurements were performed on a ZETASIZER NANO-ZS (Malvern, UK) by using a 1 mL disposable cell of a polymer solution (1 g/L) in the buffer solution. All the samples for DLS were previously filtered through a 0.45 µm filter. The water used in this research was purified using a Direct-Q Ultrapure Water System (Merck, Ltd, Darmstadt, Germany). DSC measurements were performed using a Hitachi High Tech Science XDSC7000. Scans were performed under a nitrogen atmosphere using a heating rate of 10 °C/min (from 30 to 180 °C). The glass transition temperature was determined from the second heating curve.

Synthesis of galactose-DEG-acrylamide (Gal-DEG-AAm)

2-[2-(2-propynyloxy)ethoxy]ethyl acrylamide (1.57 g, 7.96 mmol, 1 eq), galactose azide (1.96 g, 9.55 mmol, 1.2 eq), $CuSO_4$ (128 mg, 0.8 mmol, 0.1 eq), and TBTA (424.5 mg, 0.8 mmol, 0.1 eq) were dissolved in 30 mL H_2O and 60 mL MeOH. After purging nitrogen for 30 minutes at 30°C, L·Asc·Na (317 mg, 1.6 mmol, 0.2 eq) dissolved in 1 mL of water was added using a syringe. The reaction mixture was stirred at 30°C under nitrogen bubbling for 24 hours. Reaction progress was monitored by TLC (H_2O/MeCN = 1/5). The reaction solution was concentrated under reduced pressure and then filtered. The product was purified by reverse-phase silica gel chromatography (H_2O/MeOH, gradient). The product was concentrated under reduced pressure, stirred with Siliamets for 24 hours, filtered, and then concentrated under reduced pressure and lyophilized. The product was obtained as a white solid (1.68 g, 52%). **^{1}H NMR** (400 MHz, D_2O, ppm) δ: = 8.29 (s, 1H; triazole), 8.19 (s, 1H; triazole), 6.32 (dd, 1H; double bond), 6.21 (dd, 1H; double bond), 5.76 (d, 1H; anomer), 5.69 (dd, 1H; double bond), 4.72 (br, 2H; C*H*$_2$–triazole), 4.55 (dd, 1H; galactose), 4.38 (dd, 1H; galactose), 4.23 (t, 1H; galactose), 4.10–3.63 (m; galactose, ethylene glycol), 3.46 (t, 2H; C*H*$_2$–amide); **^{13}C NMR** (100 MHz, D_2O, ppm) δ: = 168.7 (C=O), 144.3 (triazole), 129.8 (double bond), 127.4 (double bond), 124.2 (triazole), 88.0 (C1, galactose), 78.3 (C5, galactose), 72.9 (C3, galactose), 69.7 (C4, galactose), 69.4 (*C*H$_2$-CH$_2$-amide), 69.0,(EG) 68.7 (EG), 68.5 (C2, galactose), 63.0 (*C*H$_2$-triazole), 60.8 (C6, galactose), 39.0 (*C*H$_2$-amide). HRMS (ESI): *m/z* calculated for [*M*+Na]$^+$, 425.17; found, 425.40.

Preparation of glycopolymers by RAFT polymerization

DMA, monomers carrying carbohydrate (GalAAm or Gal-DEG-AAm), RAFT agent (AEBCP), and initiator (AIPD) were dissolved in the solvent (DMF/water = 80: 20 vol %). The monomer concentration was 2.0 mol/L. The ratio of [RAFT]/[initiator] was 10/1. The solution was prepared in a glass tube and degassed by freeze–thaw cycles (three times). The glass tube was sealed and put in an oil bath. The reaction proceeded at 70 °C for 2 or 3 h. The reaction was stopped by exposing the solution to air. The monomer conversion was determined by ^{1}H NMR. The polymer solutions were dialyzed against Milli-Q water and lyophilized to obtain yellow solid.

Preparation of telechelic glycopolymers (linear precursors)

The glycopolymers with trithiocarbonate terminals (100 mg) were dissolved in dry DMF (4 mL) and stirred with nitrogen purging for 15 minutes. Propargyl acrylate (66 mg, 0.6 mmol), *n*-butylamine (11 mg, 0.15 mmol), and triethylamine (3 mg, 0.03 mmol) were added in that order. The mixture was stirred for 24 hours under nitrogen atmosphere. The progress of the reaction was traced by UV-vis (0.1 g/L in PBS solution). The reaction solution was dialyzed against DMSO with 500 µL of 1 M HCl(aq) for 1 day, followed by dialysis against Milli-Q water for 2 days. The purified glycopolymes were obtained as white powder by freeze-drying. The detailed reaction conditions are shown in the Supporting information (Table S2).

Cyclization of the glycopolymers by CuAAC reaction

A mixture of H_2O (150 mL) and MeCN (150 mL) dissolving $CuSO_4$ (24 mg, 0.15 mmol) was prepared in a flask and was degassed with nitrogen for 30 min (50 mL/min). The flow rate was decreased to 30 mL/min, and L·Asc·Na (40 mg, 0.2 mmol) in H_2O (1 mL) was added. To the flask, the glycopolymer aqueous solution (1 g/L) was added dropwise by syringe pump (2 mL/h). After the complete addition, the polymer solutions were kept stirring for 24 h at room temperature. The solution was concentrated by reduced pressure, and brown precipitates were removed by filtration. The filtrate was dialyzed against Milli-Q water. Siliamets was added, and the solution was scavenged for residual copper overnight. The crude products were obtained as white powder after filtration, followed by freeze-drying (Table S3-4).

Purification of the cyclic glycopolymers by recycle SEC system

Polymer purification was performed using a recycling SEC system (LaboACE LC-7080) equipped with JAIGEL-GS310/-P1. A mixture of MeOH: H_2O (4: 1) dissolving 10 mM LiBr was used as an eluent with a flow rate of 5 mL/min. The separation was conducted by injecting 3 mL of a polymer solution (10 g/L). Prior to injection, the solution was filtered through a 0.45 µm filter (PTFE). The SEC was performed under a recycling mode until the coinciding peaks were separated (detection: 220 nm). The desired fraction was collected using a fraction collector. The solution was concentrated and dialyzed against Milli-Q water. The purified products were obtained as white powder after freeze-drying (Table S3-4).

Evaluation of the interaction of the glycopolymers with a lectin by a hemagglutination inhibition assay (HI) assay

Peanut agglutinin (PNA) was desalted by use of centrifugal filter (14,000 × g for 2 times concentration spin, 1,000 × g for reverse spin) in PBS solution. PBS was added into a 96-well plate (50 µL/well) except the first lane. Desalted PNA in PBS solution (1.46 g/L, 100 µL) was added into the first line of the 96-well plate, and the solution in the first lane was diluted by two steps (50 µL). Red blood cells (RBCs) in the purchased blood cell suspension were washed by centrifugation with PBS solution three times. The concentrated RBCs were resuspended in PBS solution (0.5 v/v %), and this was injected in each well (50 µL). The 96-well plate was incubated for 1 h at room temperature, and the lowest concentration of PNA required to aggregate the RBCs was determined by visual inspection. This process was triplicated, and the average value was defined as 1HAU.

PBS was added to a 96-well plate (25 µL/well) except the first lane. Glycopolymer solution (2 g/L, 50 µL) was injected into the first lane. The solution in the first lane were twofold serially diluted (25 µL/well). PNA solution (4 HAU) was injected into each well (25 µL/well). The 96-well plate was incubated for 1 h at 25 °C. The RBC suspension was injected into each well (50 µL). The 96-well plate was incubated for 1 h at 25 °C. Precipitation of red blood cells was determined by visual inspection. This process was triplicated.

Acknowledgements

This work was financially supported by JSPS Grants-in-Aid (JP22K14728, JP22H05430, JP22H05048, JP22K19068, JP22H04553 and JP23H02015).

Conflict of interest

The authors declare no conflict of interest.

Keywords: Cyclization • click chemistry • molecular recognition • carbohydrates • polymers

[1] a) B. Bhushan, *Phil. Trans. R. Soc. A* **2009**, *367*, 1445–1486; b) A. W. Du, H. Lu, M. H. Stenzel, *Polym. Chem.* **2017**, *8*, 1750–1753; c) J. C. Cremaldi, B. Bhushan, *Beilstein J. Nanotechnol.* **2018**, *9*, 907–935; d) A. Levin, T. A. Hakala, L. Schnaider, G. J. L. Bernardes, E. Gazit, T. P. J. Knowles, *Nat. Rev. Chem.* **2020**, *4*, 615–634; e) L. M. Espinosa, W. Meesorn, D. Moatsou, C. Weder, *Chem. Rev.* **2017**, *117*, 12851–12892; f) A. Krywko-Cendrowska, S. di Leone, M. Bina, S. Yorulmaz-Avsar, C. G. Palivan, W. Meier, *Polymers* **2020**, *12*, 1003; g) M. S. Ganewatta, Z. Wang, C. Tang, *Nat. Rev. Chem.* **2021**, *5*, 753–772.

[2] a) J. Neve, J. J. haven, L. maes, T. Junkers, *Polym. Chem.* **2018**, *9*, 4692–4705. b) N. Corrigan, K. Jung, G. Moad, C. J. Hawker, K.

Matyjaszewski, C. Boyer, *Prog. Polym. Sci.* **2020**, *111*, 101311; c) S. Perrier, *Macromolecules* **2017**, *50*, 7433–7447.

[3] a) J.-F. Lutz, J.-M. Lehn, E. W. Meijer, K. Matyjaszewski, *Nat. Rev. Mater.* **2016**, *1*, 16024; b) G. Polymeropoulos, G. Zapsas, K. Ntetsikas, P. Bilalis, Y. Gnanou, N. Hadjichristidis, *Macromolecules* **2017**, *50*, 1253–1290; c) J.-F. Lutz, *ACS Macro Lett.* **2020**, *9*, 185–189; d) M. H. Barbee, Z. M. Wright, B. P. Allen, H. F. Taylor, E. F. Patteson, A. S. Knight, *Macromolecules* **2021**, *54*, 3585–3612; e) A. J. DeStefano, R. A. Segalman, E. C. Davidson, *JACS Au* **2021**, *1*, 1556–1571; f) J. L. Warren, P. A. Dykeman-Bermingham, A. S. Knight, *J. Am. Chem. Soc.* **2021**, *143*, 13228–13234; g) G. Yilmaz, V. Uzunova, R. Napier, C. R. Becer, *Biomacromolecules* **2018**, *19*, 3040–3047; h) M. Nagao, A. Yamaguchi, T. Matsubara, Y. Hoshino, T. Sato, Y. Miura, *Biomacromolecules* **2022**, *23*, 1232–1241; i) M. Nagao, Y. Miura, *ACS Macro Lett.* **2023**, *12*, 733–737.

[4] R. A. Dwek, *Chem. Rev.* **1996**, *96*, 683–720.

[5] H. Lis, N. Sharon, *Chem. Rev.* **1998**, *98*, 637–674.

[6] J. J. Lundquist, E. J. Toone, *Chem. Rev.* **2002**, *102*, 555–578.

[7] S. Cecioni, A. Imberty, S. Vidal, *Chem. Rev.* **2015**, *115*, 525–561.

[8] a) L. L. Kiessling, J. C. Grim, *Chem. Soc. Rev.* **2013**, *42*, 4476–4491; b) G. Yilmaz, C. R. Becer, *Macromol. Chem. Phys.* **2020**, *221*, 2000006; c) R. H. Bianculli, J. D. Mase, M. D. Schulz, *Macromolecules* **2020**, *53*, 9158–9186; d) M. Nagao, Y. Fujiwara, T. Matsubara, Y. Hoshino, T. Sato, Y. Miura, *Biomacromolecules* **2017**, *18*, 4385–4392; e) M. Nagao, T. Matsubara, Y. Hoshino, T. Sato, Y. Miura, *Biomacromolecules* **2019**, *20*, 2763–2769; f) M. Nagao, H. Matsumoto, Y. Miura, *Chem Asian J.* **2023**, *18*, e202300643.

[9] R. S. Kane, *Langmuir* **2010**, *26*, 8636–8640.

[10] P. I. Kitov, D. R. Bundle, *J. Am. Chem. Soc.* **2003**, *125*, 16271–16284.

[11] J. Huskens, A. Mulder, T. Auletta, C. A. Nijhuis, M. J. W. Ludden, D. N. Reinhoudt, *J. Am. Chem. Soc.* **2004**, *126*, 6784–6797.

[12] H.-X. Zhou, M. K. Gilson, *Chem. Rev.* **2009**, *109*, 4092–4107.

[13] C.-A. Chang, W. Chen, M. K. Gilson, *Proc. Natl. Acad. Sci. USA* **2007**, *104*, 1534–1539.

[14] C. Forrey, J. F. Douglas, M. K. Gilson, *Soft Matter* **2012**, *8*, 6385–6392.

[15] S. J. Irudayam, R. H. Hechman, *J. Phy. Chem. B* **2009**, *113*, 5871–5884.

[16] J. M. Fox, M. Zhao, M. J. Fink, K. Kang, G. M. Whitesides, *Annu. Rev. Biophys.* **2018**, *47*, 223–250.

[17] Y. Chen, M. S. Lord, A. Piloni, M. H. Stenzel, *Macromolecules* **2015**, *48*, 346–357.

[18] M. Nakamoto, Y. Hoshino, Y. Miura, *Biomacromolecules* **2014**, *15*, 541–547.

[19] M. Nagao, M. Kichize, Y. Hoshino, Y. Miura, *Biomacromolecules* **2021**, *22*, 3119–3127.

[20] a) F. M. Haque, S. M. Grayson, *Nat. Chem.* **2020**, *12*, 433–444; b) Z. Jia, M. J. Monteiro, *J. Polym. Sci., Part A: Polym. Chem.* **2020**, *50*, 2085–2097; c) T. Yamamoto, Y. Tezuka, *Soft Matter* **2015**, *11*, 7458–7468; d) D. Pasini, D. Takeuchi, *Chem. Rev.* **2018**, *118*, 8983−9057; e) V. Cedrati, A. Pacini, A. Nitti, A. Martínez de Ilarduya, S. Muñoz-Guerra, A. Sanyal, D. Pasini, *Polm. Chem.* **2020**, *11*, 5582−5589; f) C. L. Zaccaria, V. Cedrati, A. Pacini, E. Chiesa, A. Martínez de Ilarduya, M. Garcia-Alvarez, M. Meli, G. Colombo, D. Pasini, *Polm. Chem.* **2021**, *12*, 3784−3793; g) R.-T. Gao, L. Xu, S.-Y. Li, N. Li, Z. Chen, Z.-Q. Wu, *Chem. Eur. J.* **2023**, *29*, e202300916; h) B.-H. Duan, J.-X. Yu, R.-T. Gao, S.-Y. Li, N. Li, Z.-Q. Wu, *Chem. Commun.* **2023**, *59*, 13002–13005; i) L. Xu, B.-R. Gao, X.-H. Xu, L. Zhou, N. Li, Z. Chen, Z.-Q. Wu, *Angew. Chem. Int. Ed.* **2022**, *61*, e202204966; j) X. Hou, X. Chen, X. Gao, L. Xu, H. Zou, L. Zhou, Z.-Q. Wu, *Chin. J. Chem.* **2021**, *39*, 1181–1187.

[21] A. Zorzi, K. Deyle, C. Heinis, *Curr. Opin. Chem. Biol.* **2017**, *38*, 24–29.

[22] A. Glas, D. Bier, G. Hahne, C. Rademacher, C. Ottmann, T. N. Grossman, *Angew. Chem. Int. Ed.* **2014**, *53*, 2489–2493.

[23] A. Glas, E.-C. Wamhoff, D. M. Kruger, C. Rademacher, T. N. Grossman, *Chem. Eur. J.* **2017**, *23*, 16157–16161.

[24] L. Liu, F. Zhou, J. Hu, X. Cheng, W. Zhang, Z. Zhang, G. Chen, N. Zhou, X. Zhu, *Macromol. Rapid Commun.* **2019**, *40*, 1900223.

[25] M. Hartweg, Y. Jiang, G. Yilmaz, C. M. Jarvis, H. V.-T. Nguyen, G. A. Primo, A. Monaco, V. P. Beyer, K. K. Chen, S. Mohaptra, S. Axelrod, R. Gómez-Bombarelli, L. L. Kiessling, C. R. Becer, J. A. Johnson, *JACS Au* **2021**, *1*, 1621–1630.

[26] M. Nagao, Y. Hoshino, Y.; Miura, *Polym. Chem.* **2022**, *13*, 5453–5457.

[27] D. E. Lonsdale, C. A. Bell, M. J. Monteiro, *Macromolecules* **2010**, *43*, 3331–3339.

[28] J. P. Cohen-Addad, *Progr. NMR Spectroscopy* **1993**, *25*, 1–316.

[29] G. Hattori, Y. Hirai, M. Sawamoto, T. Terashima, *Polym. Chem.* **2017**, *8*, 7248–7259.

[30] S. Liao, L. Wei, L. A. Abriata, F. Stellacci, noparticles. *Macromolecules* **2021**, *54*, 11459–11467.

[31] L. Buts, M.-H. Dao-Thi, R. Loris, L. Wyns, M. Etzler, T. Hamelryck, *J. Mol. Biol.* **2001**, *309*, 193–201.

[32] T. R. Branson, T. E. McAllister, J. Garcia-Hartjes, M. A. Fascione, J. F. Ross, S. L. Warriner, T. Wennekes, H. Zuilhof, W. B. Turnbull, *Angew. Chem.* **2014**, *126*, 8463–8467.

[33] R. McBerney, J. P. Dolan, E. E. Cawood, M. E. Webb, W. B. Turnbull, *JACS Au* **2022**, *2*, 2038–2047.

[34] Y. Wang, J. E. Q. Quinsaat, T. Ono, M. Maeki, M. Tokeshi, T. Isono, K. Tajima, T. Satoh, S. I. Sato, Y. Miura, T. Yamamoto, *Nat. Commun.* **2020**, *11*, 6089.

[35] M. Nagao, T. Uemura, T. Horiuchi, Y. Hoshino, Y. Miura, *Chem. Commun.* **2021**, *57*, 10871–10874.

Entry for the Table of Contents

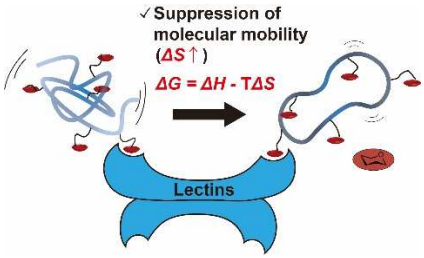

We investigated the effects of molecular mobility of the cyclic glycopolymers on their interactions with a lectin. Cyclic polymers generally have suppressed molecular mobility compared to the linear polymers due to the topology without ends of polymer structures. The suppressed mobility is expected to lead enhance the biomolecular interaction avoiding the entropy loss of the polymer conformation.